Inorganic Chemistry

Article

pubs.acs.org/IC

A Highly Selective Chemosensor for Al(III) and Zn(II) and Its Coordination with Metal Ions

Wei Cao,[†] Xiang-Jun Zheng,*[,†] Ji-Ping Sun,[†] Wing-Tak Wong,[‡] De-Cai Fang,*[,†] Jia-Xin Zhang,[†] and Lin-Pei Jin[†]

[†]Beijing Key Laboratory of Energy Conversion and Storage Materials, College of Chemistry, Beijing Normal University, Beijing 100875, People's Republic of China

[‡]Department of Applied Biology & Chemical Technology, The Hong Kong Polytechnic University, Hung Hom, Hong Kong Special Administrative Region, People's Republic of China

Supporting Information

ABSTRACT: This paper reports a fluorescence chemosensor, *N*-(benzimidazol-2-yl)salicylaldimine (H_2L), for Zn(II) and Al(III) ions. H_2L has high selectivity for Al(III) in dimethyl sulfoxide (DMSO) and for Zn(II) in *N*,*N*-dimethylformamide (DMF). In methanol, Zn(II) and Al(III) could also be distinguished by H_2L with different excitation wavelengths. The fluorescent species $[Zn(HL)(H_2O)(CH_3OH)]^+$, $[Zn(HL)(H_2O)(DMF)]^+$, $[Al(HL)_2(OH)(H_2O)]$, and $[Al(HL)(OH)_2(H_2O)(DMSO)]$ formed in solution were established by a combination of experimental and theoretical methods, including Job's plot, ^1H NMR titration, electrospray inonization mass spectrometry (ESI-MS), and B3LYP-SCRF/6-31(d) and TD-B3LYP-SCRF/6-31G* density functional theory methods. The results show that Zn(II) and Al(III) are all coordinated to the imine nitrogen atom and the hydroxyl oxygen atom from H_2L, which is the same as the M^{2+} ions in the obtained mononuclear complexes $[M(HL)_2(CH_3OH)_2]$ (where M = Cd, Ni, Co, and Mg). The detection limits of H_2L for Zn(II) were 5.98 μM in methanol and 5.76 μM in DMF, while the detection limits of H_2L for Al(III) were 3.3 μM in methanol and 5.25 μM in DMSO. Furthermore, it is also confirmed that H_2L has low toxicity for HeLa cells and could be used to detect Zn(II) and Al(III) ions in living cells by bioimaging.

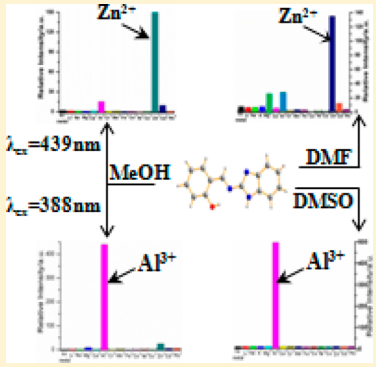

INTRODUCTION

Zinc is the second most abundant transition metal in the human body after iron, and it plays important roles in numerous biological processes including regulation of enzymes, structural cofactor in metalloproteins, neural signal transmission, and gene expression.[1] But elevated levels of Zn(II) in humans have been implicated in neurodegenerative disorders.[2] Aluminum is the third most prevalent element and the most abundant metal in the biosphere (approximately 8% of total mineral components). It is known that Al(III) is harmful to both environment and humans. Some 40% of the world's acidic soils, which are deadly to growing plants, are also affected by aluminum toxicity.[3] And even small amounts of Al^{3+} entering the human brain could cause neurodementia.[4] Therefore, it is desirable to develop some new analytical methods for detecting Zn(II) and Al(III) ions. A large number of fluorescent chemosensors for zinc or aluminum ions that employ metal−ligand coordination have been developed because of their high sensitivity and simple operation.[5] However, few fluorescent chemosensors reported can selectively sense both of them.[6] None of the bimetal [Al(III) and Zn(II)] sensors had been applied in bioimaging. A fluorescent chemosensor with different response toward multiple metal ions and with good bioimaging application is more important and would be highly desirable from the viewpoint of practical applications.

As is known, excited-state intramolecular proton transfer (ESIPT)-based chemosensors are ideal candidates for fluorescence probes.[7] They generally contain a six- and/or five-membered ring of hydrogen bonding, and proton transfer can occur, which leads to very weak or no fluorescence.[7a,8] If they are coordinated with metal ions, this proton will be removed, and thus the ESIPT process will be inhibited. Accordingly, significant fluorescence enhancement can be observed. We selected a Schiff base, *N*-(benzimidazol-2-yl)salicylaldimine (H_2L), as the target compound. It possesses an almost planar configuration[9] with excellent chromogenic unit. It can form a six-membered ring of intramolecular hydrogen-bonding configuration (Figure S1, Supporting Information), and the N and O donating atoms are favorable to probe multiple metal ions.[10] Herein, we report a chemosensor with dual selectivity for Al(III) and Zn(II) based on inhibition of ESIPT. The complex species formed in the solution were inferred through experimental and theoretical methods. Furthermore, the obtained chemosensor can be used to detect the Al(III) and Zn(II) ions in cells by bioimaging.

Received: November 8, 2013
Published: February 26, 2014

Table 1. Crystal Data and Structure Refinement Parameters of 1−4

	1	2	3	4
empirical formula	$C_{30}H_{28}CdN_6O_4$	$C_{30}H_{28}CoN_6O_4$	$C_{30}H_{28}NiN_6O_4$	$C_{30}H_{28}MgN_6O_4$
formula wt	648.98	595.51	595.29	560.89
crystal system	monoclinic	monoclinic	monoclinic	monoclinic
space group	$P2(1)/c$	$P2(1)/c$	$P2(1)/c$	$P2(1)/c$
a (Å)	6.805(6)	6.771(2)	6.761(1)	6.778(6)
b (Å)	8.767(2)	8.740(2)	8.743(2)	8.747(8)
c (Å)	23.329(3)	22.990(4)	22.919(5)	22.946(2)
α (deg)	90	90	90	90
β (deg)	99.52(2)	98.45 (4)	98.43(3)	98.47(2)
γ (deg)	90	90	90	90
V (Å^3)	1372.6(2)	1345.7(5)	1340.1(5)	1345.7(2)
Z	2	2	2	2
D_c (g·cm^{-3})	1.570	1.470	1.475	1.384
μ (mm^{-1})	0.844	0.687	0.773	0.115
$F(000)$	660	618	620	588
θ range (deg)	1.77−27.60	1.79−25.25	1.80−27.54	1.79−27.59
R_{int}	0.0476	0.0585	0.0357	0.0375
R_1, wR_2 [$I > 2\sigma(I)$]	0.0427, 0.0818	0.0447, 0.0874	0.0397, 0.0962	0.0453, 0.1065
R_1, wR_2 (all data)	0.0692, 0.0906	0.0857, 0.1039	0.0588, 0.1048	0.0776, 0.1214
GOF	1.005	1.019	1.020	1.023

Table 2. Selected Bond Distances and Angles for 1−4[a]

			Compound **1**		
Cd(1)−O(1)	2.199(2)	Cd(1)−N(1)	2.348(3)	Cd(1)−O(2)	2.320(3)
O(1)−Cd(1)−O(2)[b]	93.53(1)	O(1)−Cd(1)−O(2)	86.47(1)	O(2)−Cd(1)−N(1)	97.57(1)
O(1)−Cd(1)−N(1)[b]	96.97(9)	O(1)−Cd(1)−N(1)	83.03(9)	O(2)−Cd(1)−N(1)[b]	82.43(1)
			Compound **2**		
Co(1)−O(2)	2.080(2)	Co(1)−O(1)	2.028(2)	Co(1)−N(3)	2.253(3)
O(1)−Co(1)−O(2)	88.21(10)	O(1)−Co(1)−N(3)[c]	85.36(9)	O(1)−Co(1)−O(2)[c]	91.79(1)
O(2)−Co(1)−N(3)[c]	93.85(1)	O(2)−Co(1)−N(3)	86.15(9)	O(1)−Co(1)−N(3)	94.64(9)
			Compound **3**		
Ni(1)−N(1)	2.209(2)	Ni(1)−O(1)	2.013(2)	Ni(1)−O(2)	2.055(2)
O(1)−Ni(1)−O(2)	91.47(8)	O(1)[d]−Ni(1)−O(2)	88.53(8)	O(2)−Ni(1)−N(1)	86.86(7)
O(1)−Ni(1)−N(1)	86.26(6)	O(1)−Ni(1)−N(1)[d]	93.74(6)	O(2)−Ni(1)−N(1)[d]	93.14(7)
			Compound **4**		
Mg(1)−O(1)	2.003(1)	Mg(1)−O(2)	2.066(1)	Mg(1)−N(1)	2.287(2)
O(1)−Mg(1)−O(2)	92.29(6)	O(1)−Mg(1)−N(1)	84.29(5)	O(1)−Mg(1)−N(1)[e]	95.71(5)
O(1)−Mg(1)−O(2)[e]	87.71(6)	O(2)−Mg(1)−N(1)	85.58(5)	O(2)−Mg(1)−N(1)[e]	94.42(5)

[a]Bond distances are given in angstroms, and angles are given in degrees. [b]Symmetry code: $(-x, -y + 1, -z + 1)$. [c]Symmetry code: $(-x + 2, -y + 1, -z + 1)$. [d]Symmetry code: $(-x + 1, -y + 1, -z + 2)$. [e]Symmetry code: $(-x + 2, -y + 2, -z)$.

EXPERIMENTAL SECTION

Materials and Instrumentation. All solvents and reagents (analytical and spectroscopic grade) were used as received. Solutions of metal ions were prepared from LiCl, NaCl, KCl, $MgCl_2·6H_2O$, $CaCl_2$, $CrCl_3·6H_2O$, $MnCl_2·4H_2O$, $FeCl_3$, $CoCl_2·4H_2O$, $NiCl_2·6H_2O$, $CuCl_2·2H_2O$, $CdCl_2·2.5H_2O$, $Zn(NO_3)_2·6H_2O$, $Al(NO_3)_3·9H_2O$, and $Pb(NO_3)_2$. UV−vis absorption spectra were recorded by a UV-2450 spectrophotometer, and fluorescence spectra were recorded on a Cary Eclipse fluorescence spectrophotometer, with a quartz cuvette (path length = 1 cm). Elemental analyses were conducted with a Vario EL elemental analyzer. Fourier transform infrared (FT-IR) spectra were measured on a Avatar 360 FT-IR spectrometer as KBr pellets. ^{1}H NMR, ^{13}C NMR, and 2D spectra were obtained on a Bruker Avance III 400 MHz spectrometer. Electrospray ionization mass spectra (ESI-MS) were obtained on an LCT Premier XE time-of-flight (TOF) mass spectrometer.

Preparation of H_2L. A mixture of salicylaldehyde (0.058 g, 0.5 mmol) with 2-aminobenzimidazole (0.065g, 0.5 mmol) in 2 mL of 2-propanol was sealed in a 25 mL Teflon-lined autoclave, heated at 80 °C for 3 days, and then cooled to room temperature. Yellow stick-shaped crystals of H_2L were collected in a yield of 43.7%. Anal. Calcd for $C_{14}H_{11}N_3O$: C, 70.87; H, 4.67; N, 17.71. Found: C, 70.79; H, 4.49; N, 17.94. IR (KBr pellet, cm^{-1}) 3052 m, 2738 m, 1620 s, 1608 s, 1571 s, 1534 s, 1440 s, 1375 m, 1280 s, 1271 s, 1155 s, 772 s, 758 s, 738 vs.

Preparation of $[M(HL)_2(CH_3OH)_2]$ Complexes (M = Cd, Co, Ni, and Mg). *$[Cd(HL)_2(CH_3OH)_2]$ (**1**).* A mixture of $Cd(OAc)_2·2H_2O$ (0.027g, 0.1 mmol) and salicylaldehyde (20 μL, 0.2 mmol) with 2-aminobenzimidazole (0.027g, 0.2 mmol) in 2 mL of CH_3OH was sealed in a 25 mL Teflon-lined autoclave, heated at 80 °C for 1 day, and then cooled to room temperature. Light-yellow stick-shaped crystals were collected in a yield of 21.3% (0.014 g). Anal. Calcd for $C_{30}H_{28}CdN_6O_4$: C, 55.52; H, 4.35; N, 12.95. Found: C, 55.54; H, 4.52; N, 13.04. IR (KBr, cm^{-1}) 3060 m, 2750 m, 1603 s, 1582 s, 1526 s, 1465 s, 1434 vs, 1357 m, 1284 m, 1179 m, 1155 m, 1146 m, 745 s.

*$[Co(HL)_2(CH_3OH)_2]$ (**2**).* The Co(II) complex was synthesized similarly to the Cd complex, except that $Cd(OAc)_2·2H_2O$ was replaced by $Co(OAc)_2·6H_2O$ and the volume of methanol was changed to 7 mL, to produce deep-red stick-shaped crystals, yield 71.6% (0.044 g). Anal. Calcd for $C_{30}H_{28}CoN_6O_4$: C, 60.51; H, 4.73; N, 14.11. Found: C, 60.40; H, 4.74; N, 13.92. IR (KBr, cm^{-1}) 3058 m,

dx.doi.org/10.1021/ic402811x | Inorg. Chem. 2014, 53, 3012−3021

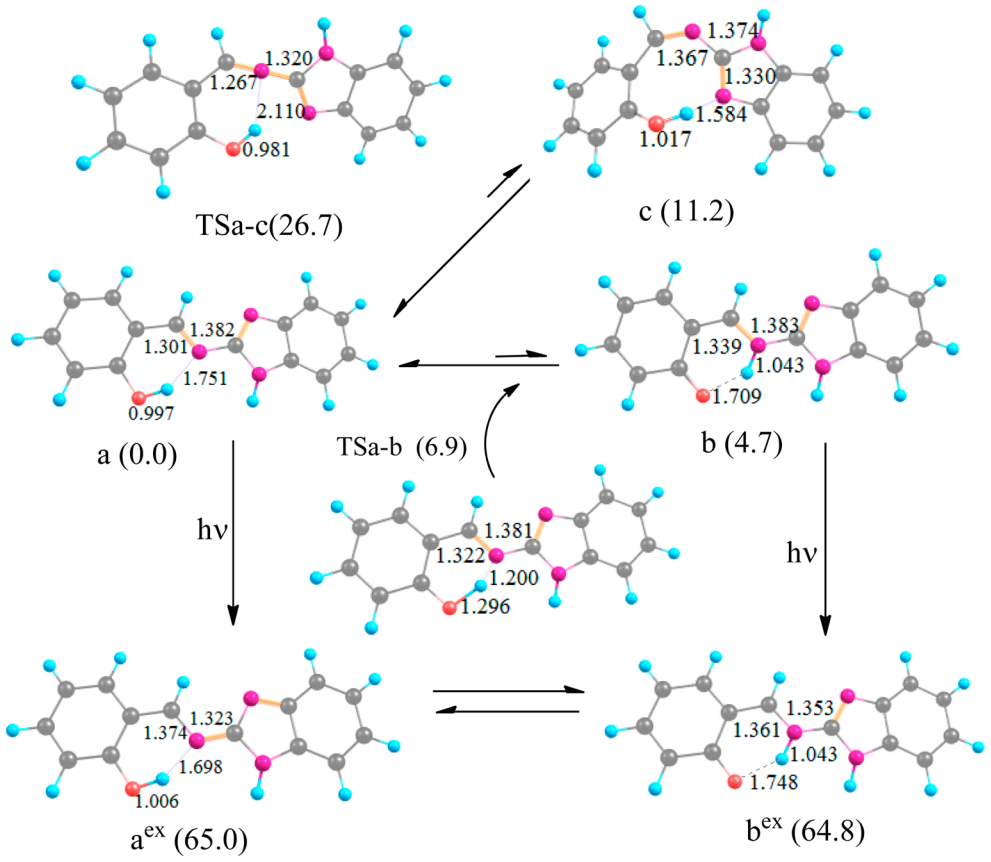

Figure 1. Hydrogen-transfer and trans−cis isomerization processes for H_2L in ground and excited states, along with relative energies (kilocalories per mole) in parentheses.

1603 s, 1588 s, 1530 m, 1468 s, 1431 vs, 1396 m, 1304 m, 1284 m, 1269 m, 1199 m, 1155 m, 1146 m, 747 s.

[Ni(HL)$_2$(CH$_3$OH)$_2$] (**3**). The Ni(II) complex was synthesized similarly to the Cd complex, except that $Cd(OAc)_2{\cdot}2H_2O$ was replaced by $Ni(OAc)_2{\cdot}4H_2O$ and the volume of methanol was changed to 7 mL, to produce green stick-shaped crystals, yield 66.9% (0.040 g). Anal. Calcd for $C_{30}H_{28}NiN_6O_4$: C, 60.53; H, 4.74; N, 14.11. Found: C, 60.13; H, 4.99; N, 13.88. IR (KBr, cm^{-1}) 3059 m, 1610 vs, 1569 m, 1481 m, 1439 m, 1304 m, 1281 m, 1273 s, 1146 m, 756 s, 746 s.

[Mg(HL)$_2$(CH$_3$OH)$_2$] (**4**). The Mg(II) complex was synthesized similarly to the Cd complex, except that $Cd(OAc)_2{\cdot}2H_2O$ was replaced by $MgCl_2{\cdot}6H_2O$ (the volume of methanol remained 2 mL), to produce yellow stick-shaped crystals, yield 14.6% (0.008 g). Anal. Calcd for $C_{30}H_{28}MgN_6O_4$: C, 64.24; H, 5.03; N, 14.98. Found: C, 64.09; H, 5.19; N, 14.60. IR (KBr, cm^{-1}) 3055 m, 1610 m, 1588 s, 1530 m, 1468 s, 1431 vs, 1304 m, 1284 m, 1269 m, 1199 m, 1155 m, 747 s.

X-ray Crystallography. Single-crystal data were collected on a Bruker Apex IICCD diffractometer with graphite monochromated Mo Kα radiation (λ) at 293 K. The structure was solved by the direct method and refined by full-matrix least-squares based on F^2 by use of the SHELX 97 program.[11] All non-hydrogen atoms were refined anisotropically. Hydrogen atoms were placed in calculated positions. Crystal data for H_2L and metal complexes (**1**−**4**) are summarized in Table S1 (Supporting Information) and Table 1, respectively. Selected bond lengths and bond angles for H_2L and complexes **1**−**4** are displayed in Table S2 (Supporting Information) and Table 2, respectively.

Calculation Methods. In this work, the quantum chemical calculations were carried out by use of the Gaussian 09 program package.[12] Possible ground-state structures have been optimized with density functional theory (DFT) at B3LYP/6-31G(d) level,[13] in which the effect of solvent has been considered using a polarized continuum model (PCM)[14] with corresponding solvent, such as methanol, *N*,*N*-dimethylformamide (DMF), and dimethyl sulfoxide (DMSO). On the basis of optimized configuration for the ground state, time-dependent (TD) DFT[15] calculations were performed by use of the B3LYP functional (TD-B3LYP-SCRF, where SCRF = self-consistent reaction field) within the adiabatic approximation to predict the excitation energies, which will provide information on fluorescence properties of studied species.

Cytotoxicity Assay. In vitro cytotoxicity was measured by a standard methylthiazolyltetrazolium (MTT) assay in HeLa cell lines. Cells growing in log phase were seeded into 96-well cell-culture plate at 1×10^4/well in 100 μL of Dulbecco's modified Eagle's medium (DMEM). H_2L was added to the wells (100 μL/well) of the treatment group, and the final concentration of H_2L ranged from 10 to 50 μM. The cells were incubated for 24 h at 37 °C under 5% CO_2. The combined MTT/phosphate-buffered saline (PBS) solution (20 μL, 5 mg/mL) was added to each well of the 96-well assay plate, and the plate was incubated for an additional 4 h. An enzyme-linked immunosorbent assay (ELISA) reader (infinite M200, Tecan, Austria) was used to measure the OD_{570} (absorbance value) of each well, referenced at 690 nm. The following formula was used to calculate the viability of cell growth: viability (%) = (mean absorbance value of treatment group/mean absorbance value of control) × 100.

Methods for Cell Imaging. HeLa cell line was cultured in DMEM. Cells were incubated with 50 μM $Zn(NO_3)_2$ or $Al(NO_3)_3$ at 37 °C for 8 h, respectively. After being washed with PBS three times to remove the remaining $Zn(NO_3)_2$ and $Al(NO_3)_3$, the cells were then incubated with 20 μM H_2L (obtained by 10^{-3} M H_2L in DMF or DMSO diluted in PBS) for 30 min at room temperature. The incubated cells were washed with PBS and mounted onto a glass slide. Fluorescent images of the mounted cells were obtained on a confocal laser scanning microscope with 405 nm excitation.

dx.doi.org/10.1021/ic402811x | Inorg. Chem. 2014, 53, 3012−3021

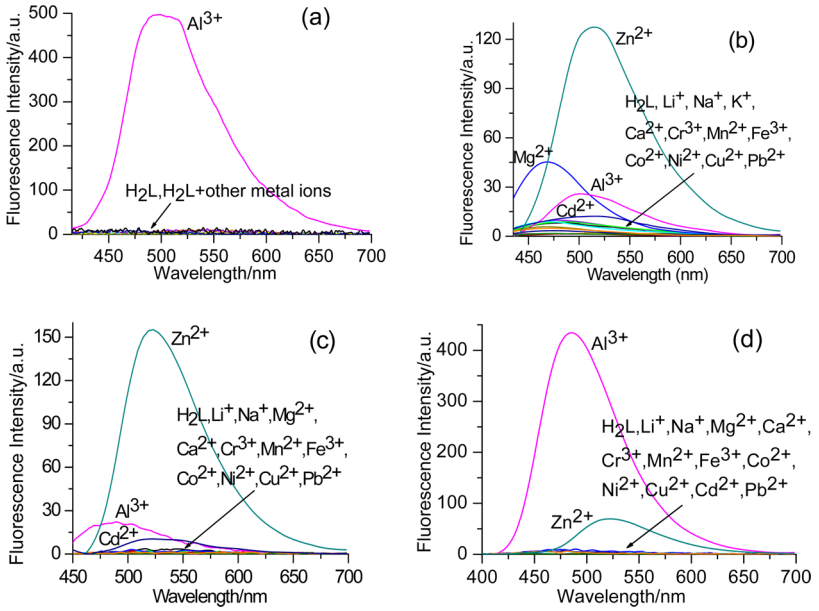

Figure 2. (a, b) Fluorescence spectra of H_2L (50 μM) upon addition of 1 equiv of metal ions in (a) DMSO (λ_{ex} = 404 nm) or (b) DMF (λ_{ex} = 421 nm). (c, d) Fluorescence spectra of H_2L (50 μM) before and after addition of 10 equiv of metal ions in methanol: excitation at (c) 439 nm or (d) 388 nm.

RESULTS AND DISCUSSION

Confirmation of Excited-State Intramolecular Proton Transfer in H_2L. In DMF, DMSO, and methanol, H_2L exhibits weak fluorescence. To determine whether ESIPT for H_2L would occur at room temperature, a theoretical calculation was first carried out. Two possible reaction paths have been explored. There are three possible isomers, labeled a, b, and c in Figure 1. As is known, the trans−cis isomerization was supposed to lead to weakened fluorescence, too.[16] Therefore, we located a ground-state trans−cis isomerization transition state (TSa−c), which is about 26.7 kcal/mol energy barrier. Obviously, it is not accessible at room temperature. We failed to locate the geometries of the excited state of c, indicating that the trans−cis isomerization would not take place at the excited-state potential energy surface. In the ground state, H_2L is mainly in the form of a in equilibrium, since the isomer of a is about 4.7 and 11.2 kcal/mol lower than those of b and c, respectively. The hydrogen-transfer process from a to b needs to overcome an energy barrier 6.9 kcal/mol, but its reverse process requires only 2.2 kcal/mol. However, in the excited state of H_2L, the energy of b is about 0.2 kcal/mol lower than that of a, meaning that such species with higher energy will lead to the hydrogen-transfer process taking place more easily, which suggests that ESIPT might occur and lead to weakened fluorescence of H_2L. Once H_2L is coordinated to a metal ion, inhibition of the ESIPT process results in great fluorescence enhancement.

Selectivity of H_2L for Metal Ions. The fluorescence responses of H_2L to metal ions are significantly affected by solvents (Figure 2). In DMSO (Figure 2a), upon addition of Li(I), Na(I), K(I), Ca(II), Mg(II), Cr(III), Mn(II), Fe(III), Co(II), Ni(II), Cu(II), Zn(II), oe Pb(II) to H_2L, no obvious fluorescence response could be observed. However, addition of Al(III) to a DMSO solution of H_2L resulted in 62-fold fluorescence enhancement at 510 nm, indicating high selectivity of H_2L for Al(III) ions in DMSO with τ = 6.3 ns. In DMF, addition of Zn(II) resulted in turn-on fluorescence with 17-fold enhancement of the emission intensity at 515 nm with τ = 0.35 ns (Figure 2b). Other metal ions, such as Li(I), Na(I), K(I), Ca(II), Cr(III), Mn(II), Fe(III), Co(II), Ni(II), Cu(II), and Pb(II), caused negligible fluorescence response, while Mg(II) and Al(III) showed weak fluorescence enhancement. When methanol was chosen as solvent, a different phenomenon could be observed. After excitation at 439 nm, the fluorescence intensity at 525 nm was remarkably enhanced (47-fold) upon addition of Zn(II) with τ = 0.36 ns (Figure 2c), while upon binding with Al(III), it showed a large blue shift band with 181-fold enhancement at 485 nm when excited at 388 nm with τ = 11.7 ns (Figure 2d). This drastic blue shift could be attributed to stronger perturbation of the electric structure of Al(III) complex, resulting in the larger solvochromic shift.[17,18] When either 439 or 388 nm was used as excitation wavelength, addition of other metal ions exhibited negligible changes in the fluorescence spectra, showing an excitation wavelength-dependent fluorescence response of H_2L for Al(III) and Zn(II). In the three solvents, fluorescence enhancement may all result from the inhibition of ESIPT of H_2L by the formation of complexes between H_2L and Al(III) or Zn(II).

To investigate the selectivity of H_2L for Zn(II) and Al(III) over a range of various metal cations [Li(I), Na(I), K(I), Ca(II), Mg(II), Cr(III), Mn(II), Fe(III), Co(II), Ni(II), Cu(II), Cd(II), and Pb(II)], we carried out competition experiments in DMSO, DMF, and methanol (Figures S2 and S3, Supporting Information). From the bar diagrams, the selectivity of H_2L for Al(III) in DMSO and methanol and for Zn(II) in DMF and methanol are similar, respectively. Except for Fe(III), Cu(II), and Pb(II), a background of competing metal ions showed no interference with the detection of Al(III) ion in DMSO and methanol. And in the case of Fe(III), Cu(II) and Pb(II), the fluorescence intensities still showed a sufficient turn-on ratio for the detection of Al(III). While compared with Al(III) ion, H_2L showed less selectivity for Zn(II). It is well-known that Zn(II) chemosensors may be detrimentally affected by interference from other cations, especially Cu(II).[2a,19] The

dx.doi.org/10.1021/ic402811x | Inorg. Chem. 2014, 53, 3012−3021

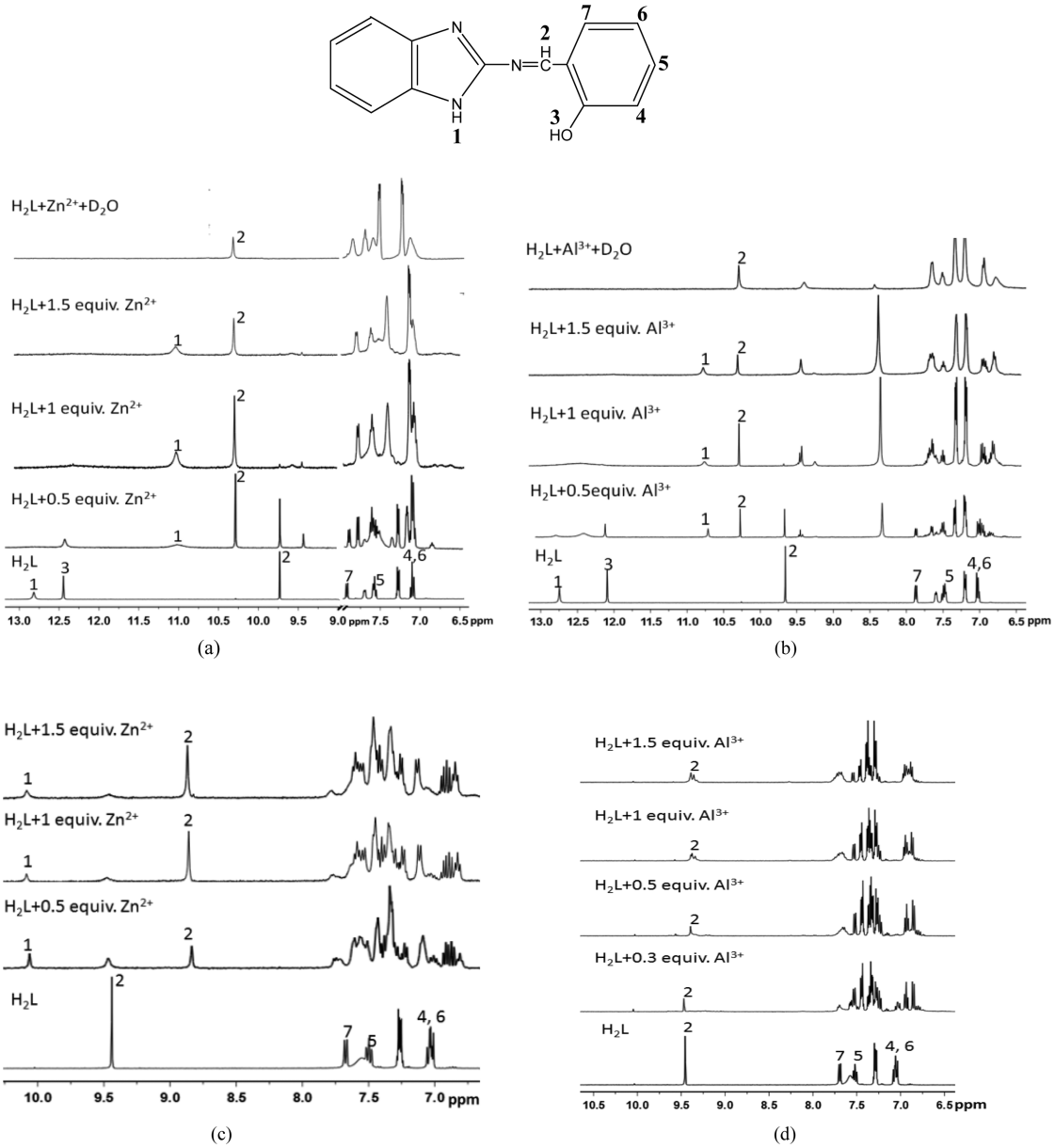

Figure 3. ^{1}H NMR spectra of H_2L with and without Zn(II) or Al(III) in (a) DMF-d_7, (b) DMSO-d_6, and (c, d) methanol-d_4.

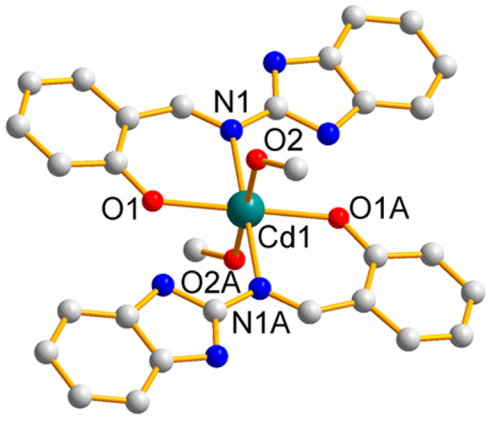

Figure 4. Crystal structure of Cd complex. The related coordination atoms are labeled out. All H atoms are omitted for clarity. Symmetry code: (A) $-x$, $1-y$, $1-z$.

paramagnetic metal cations Cr(III), Fe(III), Co(II), and Ni(II) resulted in fluorescence quenching.

Binding Mode and Composition of Metal Species. To understand the interactions between H_2L and metal ions, Job's plots and ^{1}H NMR for H_2L sensing Zn(II) or Al(III) in three solvents were carried out. Job's plot indicates a binding stoichiometry of 1:1 for H_2L to Zn(II) and Al(III) in DMF and DMSO, respectively (Figure S4a,b, Supporting Information). In methanol the binding stoichiometry for H_2L to Zn(II) and Al(III) confirmed by Job's plot is 1:1 and 2:1 (Figure S4c,d, Supporting Information), respectively. Assignments of signals of H_2L were established by ^{1}H NMR, ^{13}C NMR, and 2D NMR spectra in DMF-d_7, DMSO-d_6, and methanol-d_4 (Figures S5, S6, and S7 in Supporting Information), respectively. The binding mode of H_2L was proved by ^{1}H NMR experiments (Figure 3). In DMF-d_7 (Figure 3a), the proton of phenolic O–H (H_3) at 12.43 ppm disappeared upon addition of 1 equiv of Zn(II), suggesting the binding of oxygen atom to Zn(II) ion. At the same time, the proton of HC═N (H_2) shifted downfield

dx.doi.org/10.1021/ic402811x | Inorg. Chem. 2014, 53, 3012−3021

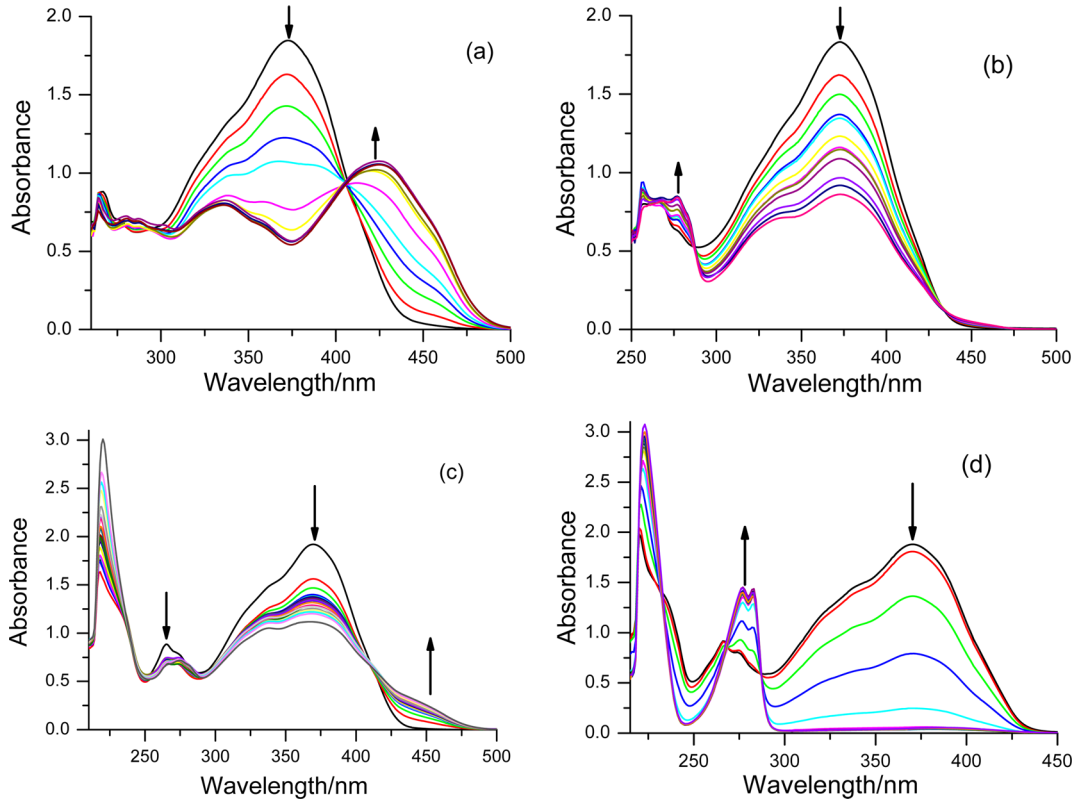

Figure 5. (a) Absorption spectra of H_2L (0.1 mM) upon addition of Zn(II) (0−1.0 equiv) in DMF. (b) UV−vis spectra changes of 0.1 mM H_2L after addition of Al(III) ions (0−2.0 equiv) in DMSO. (c) UV−vis spectra changes of 0.1 mM H_2L after addition of Zn(II) ions (0−3.0 equiv) in CH_3OH. (d) UV−vis spectra changes of 0.1 mM H_2L after addition of Al(III) ions (0−1.5 equiv) in CH_3OH.

from 9.73 to 10.45 ppm by N−metal coordination. Meanwhile, the N−H (H_1) proton at benzimidazole did not disappear and shifted upfield from 12.82 to 11.20 ppm, which means that this nitrogen atom cannot bind with metal ion. A weak signal located at 9.41 ppm disappeared upon addition of D_2O, possibly indicating a signal of active hydrogen from coordinated water molecule. Similarly, in DMSO-d_6 (Figure 3b), the signals of H_1, H_2, and H_3 of H_2L were changed upon addition of Al(III). H_1 shifted upfield from 12.73 to 10.70 ppm, H_2 shifted downfield from 9.73 to 10.45 ppm, and H_3 at 12.08 ppm disappeared. However, different from that in DMF-d_7 for Zn(II), there were two new signals observed at 8.34 and 9.40 ppm that became very weak upon addition of D_2O. This suggests that they are signals of active hydrogen, OH^- and H_2O, which may result from the fact that Al(III) is easily hydrolyzed.[20] In either DMF-d_7 or DMSO-d_6, upon further addition of metal ions (>1.0 equiv), there was no hydroxyl proton signal and the proton shift remained the same, which confirms 1:1 complexation between Zn(II) and H_2L in DMF and between Al(III) and H_2L in DMSO. The changes of ^1H NMR signals for H_2L with and without Zn(II) or Al(III) in methanol-d_4 showed the formation of Zn(II)−HL and Al(III)−HL complexes (Figure 3c,d). There were no noticeable changes observed in the peak position upon addition of >1.0 equiv of Zn(II) to H_2L and addition of >2.0 equiv of H_2L to Al(III), indicating the formation of Zn(II)−HL (1:1) and Al(III)−$(HL)_2$ (1:2) species.

There are four potential coordination sites for H_2L: three nitrogen atoms and one oxygen atom. To confirm the coordination mode of H_2L, we tried to obtain crystals of its complexes with metal ions such as Zn(II), Al(III), Cd(II), Ni(II), Co(II), and Mg(II). Only the crystals of Cd(II), Ni(II), Co(II), and Mg(II) complexes were obtained. Single-crystal X-ray diffraction revealed that the four complexes are isostructural, so only the Cd(II) complex (**1**) will be described. The Cd(II) complex is a centrosymmetric mononuclear complex crystallizing in the monoclinic system and $P2_1/c$ space group. The central Cd(II) ion is coordinated with two deprotonated HL and two methanol molecules in an octahedral coordination geometry (Figure 4). The two deprotonated ligands are almost coplanar. The ligand HL chelates to the metal ion in bidentate mode with an imine nitrogen atom and a hydroxyl oxygen atom, which is the same as we deduced from ^1H NMR of the fluorescent species.

In order to understand the species formed in solution in detail, electrospray ionization mass spectra were also measured. As shown in Figure S8 (Supporting Information), upon addition of Zn(II) the mass spectrum of H_2L in methanol exhibited intense peaks at m/z = 350.06, corresponding to the ion $[Zn(HL)(H_2O)(CH_3OH)]^+$ (calcd m/z 350.05). When Al(III) was introduced to H_2L in methanol, a peak at m/z = 557.05 (calcd m/z 557.14) corresponding to $Na^+[Al(HL)_2(OH)(H_2O)]$ was present, indicating the complexes formed between H_2L and metal ions Zn(II) and Al(III) with 1:1 and 2:1 stoichiometry, respectively. Meanwhile, the ESI mass spectra of Zn(II) in DMF and Al(III) in DMSO were in agreement with 1:1 stoichiometry (Figure S9, Supporting Information). Peaks at m/z = 391.11 in DMF and m/z = 416.05 in DMSO were attributed to $[Zn(HL)(H_2O)(DMF)]^+$ (calcd m/z 391.07) and $Na^+[Al(HL)(DMSO)(OH)_2(H_2O)]$ (calcd m/z 416.08), respectively. The four different Zn(II) and Al(III) complexes with H_2L were formed in different solvents.

dx.doi.org/10.1021/ic402811x | Inorg. Chem. 2014, 53, 3012−3021

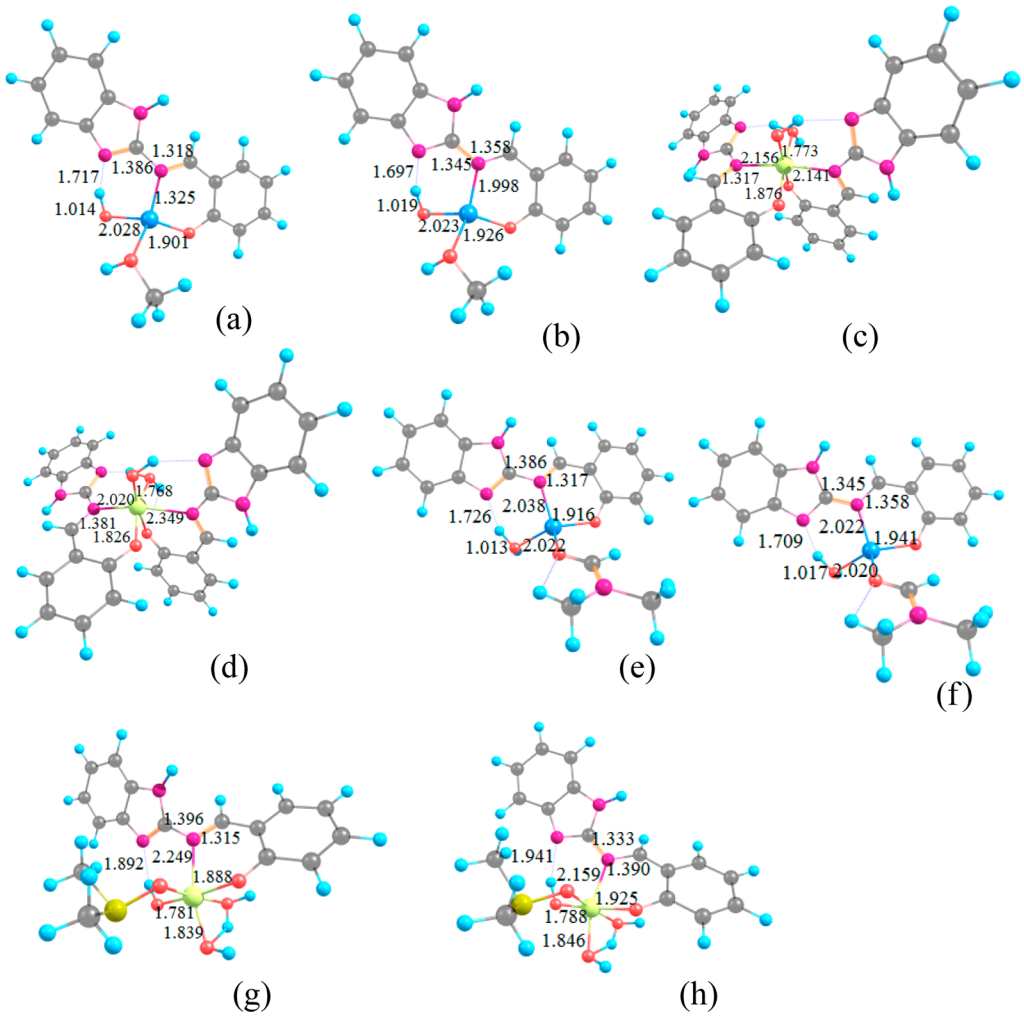

Figure 6. Main geometric parameters (in angstroms) for optimized stationary points: $[Zn(HL)(H_2O)[CH_3OH]]^+$, (a) ground and (b) excited; $[Al(HL)_2(OH)(H_2O)]$, (c) ground and (d) excited; $[Zn(HL)(H_2O)(DMF)]^+$, (e) ground and (f) excited; and $[Al(HL)(OH)_2(H_2O)(DMSO)]$, (g) ground and (h) excited.

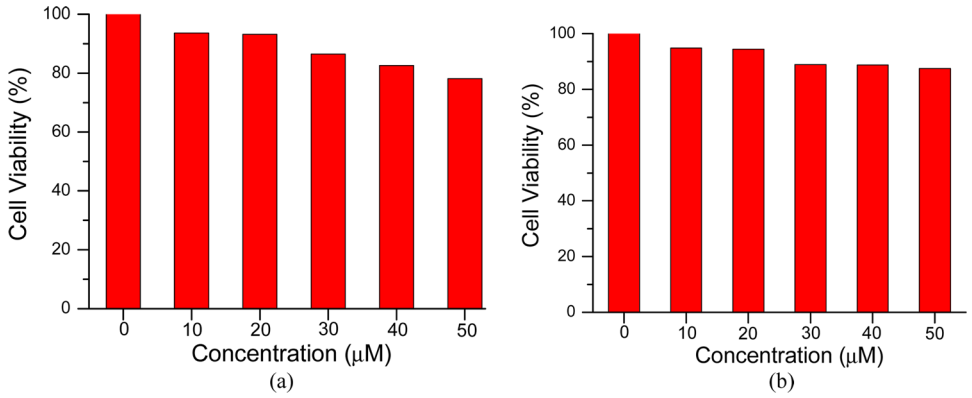

Figure 7. Cell viability values (%) estimated by MTT proliferation test versus concentrations of H_2L after 24 h incubation at 37 °C in (a) DMF/H_2O or (b) DMSO/H_2O.

The Zn(II) ion is four-coordinated while the Al(III) ion is six-coordinated. The Al(III) ion tends to hydrolyze to form hydrolyzed species in the formation of Al(III) complexes. CH_3OH, DMSO, and DMF can act as donors. The formation and composition of the Zn(II) and Al(III) complexes depend on coordination geometry and acid−base characteristics of the metal ions and donor strength of the solvent.

Sensitivity of H_2L for Metal Ions. H_2L sensor was titrated with Zn(II) and Al(III) in three solvents. The absorption spectrum of H_2L exhibited a band centered at 375 nm, which arises from $\pi-\pi^*$ transition of H_2L. This band decreased with a concomitant increase in a new peak upon addition of increasing amounts of metal ions. The well-defined isosbestic points observed are also indicative of a clear conversion of H_2L into

dx.doi.org/10.1021/ic402811x | Inorg. Chem. 2014, 53, 3012−3021

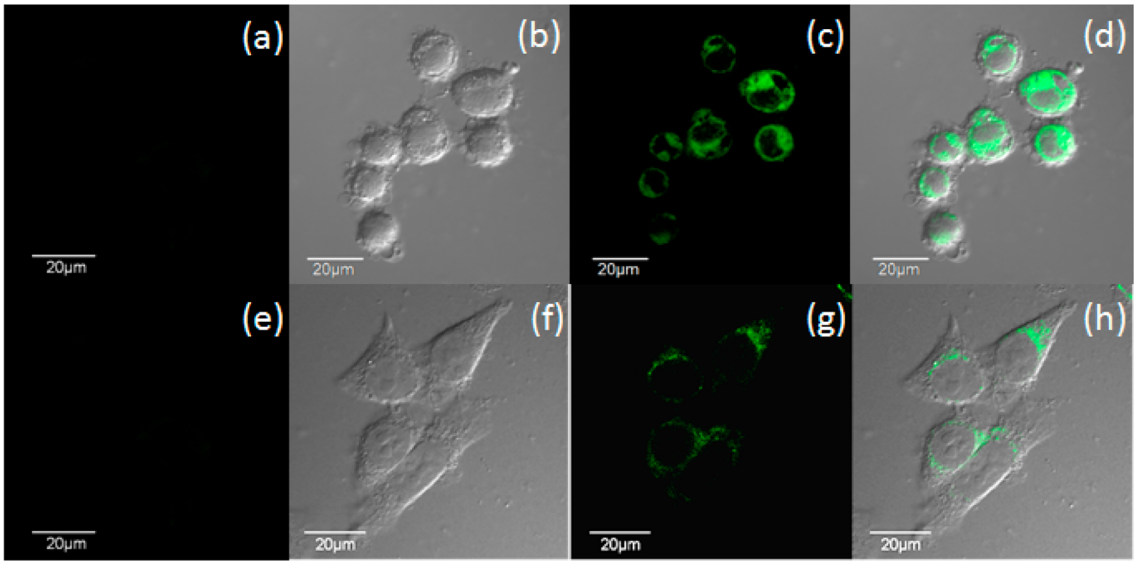

Figure 8. Confocal fluorescence and bright-field images of HeLa cells: (a, e) cells supplemented with 20 μM H_2L in growth medium for 30 min; (b, f) bright-field image of cells incubated with (b) H_2L and $Zn(NO_3)_2$ or (f) H_2L and $Al(NO_3)_3$; (c, g) cells shown in panels b and f; (d) overlay image of panels b and c (λ_{ex} = 405 nm); (h) overlay image of panels f and g (λ_{ex} = 405 nm).

M^{n+} complex (Figure 5). We also evaluated changes in fluorescence of H_2L upon treatment with Zn(II) and Al(III) ions. In DMF, when H_2L was titrated with Zn(II) (Figure S10, Supporting Information), a binding constant (log K_a) of 4.4 was obtained from a nonlinear least-squares fit according to a 1:1 binding stoichiometry (Figure S11a) and the detection limit of H_2L for Zn(II) was 5.76 μM (Figure S11b, Supporting Information).[21] Similarly, in methanol the binding constant (log K_a) and detection limit of H_2L for Zn(II) were 4.9 and 5.98 μM, correspondingly (Figure S12, Supporting Information). In DMSO, the binding constant (log K_a) of H_2L for Al(III) was 4.3 (Figure S13a) and the detection limit of H_2L for Al(III) was found to be 5.25 μM (Figure S13b, Supporting Information). In methanol, Al(III) could be detected at least to 3.3 μM based on the 3σ/slope.[21] The binding constant (log K_a) of H_2L for Al(III) was 8.08 (Figure S14, Supporting Information).[3d]

Geometry and Emission Properties of Metal Species. In order to uncover the fluorescence properties for the studied species, B3LYP-SCRF/6-31G(d) and TD-B3LYP-SCRF/6-31G* methods have been employed to characterize the energies, structures, frequencies, and spectroscopic properties (Figure 6; Tables S3−S6, Supporting Information). For $[Zn(HL)(H_2O)(CH_3OH)]^+$, the excitation and fluorescence wavelengths were 409 and 494 nm, respectively, which correspond to highest unoccupied molecular orbital (HOMO) → lowest unoccupied molecular orbital (LUMO) (CH═N $\pi \rightarrow \pi^*$) and LUMO → HOMO (CH═N $\pi^* \rightarrow \pi$), in line with the change (1.318 → 1.358 Å) of CH═N bond length from the ground state to the excited state. For $[Zn(HL)(H_2O)(DMF)]^+$, the corresponding values were 410 (excitation) and 493 nm (fluorescence), and the change of bond length CH═N was 1.317 → 1.358 Å. The calculated Stokes shift of 85 nm for $[Zn(HL)(H_2O)(CH_3OH)]^+$ and 83 nm for $[Zn(HL)(H_2O)(DMF)]^+$ are in line with the lengthening of the CH═N bond length (0.04 Å). The observed maximum emission positions for $[Zn(HL)(H_2O)(CH_3OH)]^+$ in CH_3OH and $[Zn(HL)(H_2O)(DMF)]^+$ in DMF were 525 and 515 nm, respectively. The fluorescence peak for $[Zn(HL)(H_2O)(CH_3OH)]^+$ was red-shifted. This phenomenon can be attributed to the fact that the magnitude of the energy difference between the ground and excited states of the sensor is significantly influenced by solvent coordination and solute−solvent interaction, such as hydrogen bonding. For $[Al(HL)_2(OH)(H_2O)]$ and $[Al(HL)(OH)_2(H_2O)(DMSO)]$, the shifts of CH═N bond length become 1.317 → 1.381 Å and 1.315 → 1.390 Å, respectively. The calculated excitation and emission wavelengths are 397 and 483 nm and 392 and 525 nm, respectively, Calculated data for the four metal complexes show a similar trend with the experimental results.

Cell Toxicity of H_2L and Its Bioimaging with Metal Ions. The cellular toxicity of H_2L to HeLa cells in DMF/H_2O and DMSO/H_2O was determined by MTT assay with the concentration of H_2L ranging from 10 to 50 μM (Figure 7). Upon incubation for 24 h of 20 μM H_2L (a concentration that was used for confocal imaging studies), the cellular viabilities were estimated to be 93% and 94% in DMF/H_2O and DMSO/H_2O, respectively. The results indicate that H_2L has low toxicity for HeLa cells.

Then experiments were conducted to determine whether H_2L can be used to fluorescently visualize intracellular Zn(II) and Al(III). For this purpose, HeLa cells were first incubated with $Zn(NO_3)_2$ or $Al(NO_3)_3$ for 8 h and then treated with a final concentration of 20 μM H_2L for 30 min before imaging. When cells were exposed to H_2L, no fluorescence was observed, while strong fluorescence was observed in cells exposed to H_2L and Zn(II) or to H_2L and Al(III) ions (Figure 8). These results demonstrate that H_2L is permeable to HeLa cells and binds intracellular Zn(II) and Al(III), thus emitting fluorescence upon binding the metal ions.

■ CONCLUSIONS

The fluorescent chemosensor *N*-(benzimidazol-2-yl)-salicylaldimine (H_2L) displayed excellent selectivity for Zn(II) and Al(III) over a number of metal ions in DMF, DMSO, and methanol. It can be used to detect intracellular Al(III) and Zn(II) ions by living cell imaging. Calculations show that the mechanism of fluorescence enhancement of the metal species is

dx.doi.org/10.1021/ic402811x | Inorg. Chem. 2014, 53, 3012−3021

based on inhibition of the ESIPT process of H_2L when it is coordinated to metal ions. The formation and fluorescent behaviors of Zn(II)−HL and Al(III)−HL complexes $[Zn(HL)(H_2O)(CH_3OH)]^+$, $[Zn(HL)(H_2O)(DMF]^+$, $[Al(HL)_2(OH)(H_2O)]$, and $[Al(HL)(OH)_2(H_2O)(DMSO)]$ are solvent-dependent. The solvent effect on fluorescence is possibly attributed to solvent polarity, viscosity, and hydrogen-bonding ability. The coordination modes of H_2L with Al(III) and Zn(II) to form metal complexes in DMSO, DMF, and methanol are the same as those in $[M(HL)_2(CH_3OH)_2]$ complexes (M = Cd, Ni, Co, and Mg). Our work shows that nitrogen- and oxygen-containing Schiff bases can serve as a platform to explore fluorescent chemosensors for multiple metal ions.

■ ASSOCIATED CONTENT

Supporting Information

Fourteen figures and six tables showing crystal data and structure of H_2L; Job's plots; 2D NMR spectra of H_2L in DMSO-d_6, DMF-d_7, and methanol-d_4; ESI mass spectra; fluorescence titration profiles; Benesi−Hildebrand plots; profiles for competitive experiments; optimized Cartesian coordinates; and energies and frequencies for H_2L and fluorescent species (PDF). X-ray crystallographic data (CIF). This material is available free of charge via the Internet at http://pubs.acs.org.

■ AUTHOR INFORMATION

Corresponding Authors

*E-mail: xjzheng@bnu.edu.cn.
*E-mail: dcfang@bnu.edu.cn.

Notes

The authors declare no competing financial interest.

■ ACKNOWLEDGMENTS

This work is supported by the National Natural Science Foundation of China (20971015), the Hong Kong Scholar Program, and the Fundamental Research Funds for the Central Universities.

■ REFERENCES

(1) (a) Frederickson, C. J.; Koh, J.-Y.; Bush, A. I. *Nat. Rev. Neurosci.* **2005**, *6*, 449−462. (b) Berg, J. M.; Shi, Y. G. *Science* **1996**, *271*, 1081−1085. (c) Frausto da Silva, J. J. R.; Williams, R. J. P. In *The Biological Chemistry of the Elements*; Oxford University Press: New York, 2001; pp 315−335. (d) Dhanasekaran, M.; Negi, S.; Sugiura, Y. *Acc. Chem. Res.* **2006**, *39*, 45−52. (e) Sousa, S. F.; Fernandes, P. A.; Ramos, M. J. *J. Am. Chem. Soc.* **2007**, *129*, 1378−1385. (f) Mott, D. D.; Benveniste, M.; Dingledine, R. J. *J. Neurosci.* **2008**, *28*, 1659−1671.

(2) (a) Bush, A. I.; Pettingell, W. H.; Multhaup, G.; Paradis, M.; Vonsattel, J.-P.; Gusella, J. F.; Beyreuther, K.; Masters, C. L.; Tanzi, R. E. *Science* **1994**, *265*, 1464−1467. (b) Bush, A. I. *Trends Neurosci.* **2003**, *26*, 207−214. (c) Noy, D.; Solomonov, I.; Sinkevich, O.; Arad, T.; Kjaer, K.; Sagi, I. *J. Am. Chem. Soc.* **2008**, *130*, 1376−1383.

(3) (a) Flaten, T. P.; Ødegård, M. *Food Chem. Toxicol.* **1988**, *26*, 959−960. (b) Yokel, R. A. *NeuroToxicology* **2000**, *21*, 813−828. (c) Ren, J.; Tian, H. *Sensors* **2007**, *7*, 3166−3178. (d) Kim, S. H.; Choi, H. S.; Kim, J.; Lee, S. J.; Quang, D. T.; Kim, J. S. *Org. Lett.* **2010**, *12*, 560−563.

(4) (a) Burwen, D. R.; Olsen, S. M.; Bland, L. A.; Arduino, M. J.; Reid, M. H.; Jarvis, W. R. *Kidney Int.* **1995**, *48*, 469−474. (b) Fasman, G. D. *Coord. Chem. Rev.* **1996**, *149*, 125−165. (c) Nayak, P. *Environ. Res.* **2002**, *89*, 101−115. (d) Cronan, C. S.; Walker, W. J.; Bloom, P. R. *Nature* **1986**, *324*, 140−143. (e) Berthon, G. *Coord. Chem. Rev.* **2002**, *228*, 319−341. (f) Martin, R. B. *Acc. Chem. Res.* **1994**, *27*, 204−210. (g) Bielarczyk, H.; Jankowska, A.; Madziar, B.; Matecki, A.; Michno, A.; Szutowicz, A. *Neurochem. Int.* **2003**, *42*, 323−331. (h) Yousef, M. I.; EI-Morsy, A. M.; Hassan, M. S. *Toxicology* **2005**, *215*, 97−107.

(5) (a) Xu, Z.; Baek, K.; Kim, H. N.; Cui, J.; Qian, X.; Spring, D. R.; Shin, I.; Yoon, J. *J. Am. Chem. Soc.* **2010**, *132*, 601−610. (b) Du, P.; Lippard, S. J. *Inorg. Chem.* **2010**, *49*, 10753−10755. (c) Xu, Z. C.; Yoon, J.; Spring, D. R. *Chem. Soc. Rev.* **2010**, *39*, 1996−2006. (d) Kwon, J. E.; Lee, S.; You, Y.; Baek, K. H.; Ohkubo, K.; Cho, J.; Fukuzumi, S.; Shin, I.; Park, S. Y.; Nam, W. *Inorg. Chem.* **2012**, *51*, 8760−8774. (e) Kim, S.; Noh, J. Y.; Kim, K. Y.; Kim, J. H.; Kang, H. K.; Nam, S. W.; Kim, S. H.; Park, S.; Kim, C.; Kim, J. *Inorg. Chem.* **2012**, *51*, 3597−3602. (f) Maity, D.; Govindaraju, T. *Chem. Commun.* **2010**, *46*, 4499−4501. (g) Maity, D.; Govindaraju, T. *Inorg. Chem.* **2010**, *49*, 7229−7231. (h) Sahana, A.; Banerjee, A.; Lohar, S.; Sarkar, B.; Mukhopadhyay, S. K.; Das, D. *Inorg. Chem.* **2013**, *52*, 3627−3633. (i) Woodroofe, C. C; Lippard, S. J. *J. Am. Chem. Soc.* **2003**, *125*, 11458−11459. (j) Maruyama, S.; Kikuchi, K.; Hirano, T.; Urano, Y.; Nagano, T. *J. Am. Chem. Soc.* **2002**, *124*, 10650−10651. (k) Arduini, M.; Felluga, F.; Mancin, F.; Rossi, P.; Tecilla, P.; Tonellato, U.; Valentinuzzi, N. *Chem. Commun.* **2003**, *39*, 1606−1607. (l) Sun, X.; Wang, Y. W.; Peng, Y. *Org. Lett.* **2012**, *14*, 3420−3423. (m) Shi, X. Y.; Wang, H.; Han, T. Y. *J. Mater. Chem.* **2012**, *22*, 19296−19302.

(6) (a) Maity, D.; Govindaraju, T. *Chem. Commun.* **2012**, *48*, 1039−1041. (b) Shellaiah, M.; Wu, Y. H.; Lin, H. C. *Analyst* **2013**, *138*, 2931−2942.

(7) (a) Liu, Z. P.; He, W. J.; Guo, Z. J. *Chem. Soc. Rev.* **2013**, *42*, 1568−1600. (b) Yuan, L.; Lin, W. Y.; Zheng, K. B.; Zhu, S. S. *Acc. Chem. Res.* **2013**, *46*, 1462−1473.

(8) (a) Wu, J. S.; Liu, W. M.; Ge, J. C.; Zhang, H. Y.; Wang, P. F. *Chem. Soc. Rev.* **2011**, *40*, 3483−3495. (b) Henary, M. M.; Fahrni, C. J. *J. Phys. Chem. A* **2002**, *106*, 5210−5220.

(9) Murali, M.; Nayak, S.; Costa, J. S.; Ribas, J.; Mutikainen, I.; Turpeinen, U.; Clémancey, M.; Garcia-Serres, R.; Latour, J. M.; Gamez, P.; Blondin, G.; Reedijk, J. *Inorg. Chem.* **2010**, *49*, 2427−2434.

(10) (a) Aline, S.; Taniguchi, T.; Saiki, T.; Nabeshima, T. *J. Am. Chem. Soc.* **2005**, *127*, 540−541. (b) Neupane, L. N.; Park, J. Y.; Park, J. H.; Lee, K. H. *Org. Lett.* **2013**, *15*, 254−257.

(11) Sheldrick, G. M. *SHELXS-97, Program for solution of crystal structures*, University of Göttingen, Germany, 1997.

(12) Frisch, M. J.; Trucks, G. W.; Schlegel, H. B.; Scuseria, G. E.; Robb, M. A.; Cheeseman, J. R.; Scalmani, G.; Barone, V.; Mennucci, B.; Petersson, G. A.; Nakatsuji, H.; Caricato, M.; Li, X.; Hratchian, H. P.; Izmaylov, A. F.; Bloino, J.; Zheng, G.; Sonnenberg, J. L.; Hada, M.; Ehara, M.; Toyota, K.; Fukuda, R.; Hasegawa, J.; Ishida, M.; Nakajima, T.; Honda, Y.; Kitao, O.; Nakai, H.; Vreven, T.; Montgomery, J. A., Jr.; Peralta, J. E.; Ogliaro, F.; Bearpark, M.; Heyd, J. J.; Brothers, E.; Kudin, K. N.; Staroverov, V. N.; Keith, T.; Kobayashi, R.; Normand, J.; Raghavachari, K.; Rendell, A.; Burant, J. C.; Iyengar, S. S.; Tomasi, J.; Cossi, M.; Rega, N.; Millam, J. M.; Klene, M.; Knox, J. E.; Cross, J. B.; Bakken, V.; Adamo, C.; Jaramillo, J.; Gomperts, R.; Stratmann, R. E.; Yazyev, O.; Austin, A. J.; Cammi, R.; Pomelli, C.; Ochterski, J. W.; Martin, R. L.; Morokuma, K. V.; Zakrzewski, G.; Voth, G. A.; Salvador, P.; Dannenberg, J. J.; Dapprich, S.; Daniels, A. D.; Farkas, O.; Foresman, J. B.; Ortiz, J. V.; Cioslowski, J.; Fox, D. J. *Gaussian 09*, Gaussian, Inc., Wallingford, CT, 2010.

(13) Becke, A. D. *J. Chem. Phys.* **1982**, *65*, 239−245.

(14) (a) Cossi, M.; Barone, V.; Cammi, R.; Tomasi, J. *Chem. Phys. Lett.* **1996**, *255*, 327−335. (b) Scalmani, G.; Frisch, M. J. *J. Chem. Phys.* **2010**, *132*, No. 114110.

(15) (a) Furche, F.; Ahlrichs, R. *J. Chem. Phys.* **2002**, *117*, 7433−7447. (b) Scalmani, G.; Frisch, M. J. *J. Chem. Phys.* **2006**, *124*, No. 094107.

(16) Wu, J. S.; Liu, W. M.; Zhuang, X. Q.; Wang, F.; Wang, P. F.; Tao, S. L.; Zhang, X. H.; Wu, S. K.; Lee, S. T. *Org. Lett.* **2007**, *9*, 33−36.

(17) de Silva, A. P.; Gunaratne, H. Q. N.; Gunnlaugsson, T.; Huxley, A. J. M.; McCoy, C. P.; Rademacher, J. T.; Rice, T. E. *Chem. Rev.* **1997**, *97*, 1515−1566.

(18) Houmøller, J.; Wanko, M.; Støchkel, K.; Rubio, A.; Nielsen, S. B. *J. Am. Chem. Soc.* **2013**, *135*, 6818−6821.
(19) Teolato, P.; Rampazzo, E.; Arduini, M.; Mancin, F.; Tecilla, P.; Tonellato, U. *Chem.—Eur. J.* **2007**, *13*, 2238−2245.
(20) Stavitski, E.; Goesten, M.; Juan-Alcañiz, J.; Martinez-Joaristi, A.; Serra-Crespo, P.; Petukhov, A.; Gascon, J.; Kapteijn, F. *Angew. Chem., Int. Ed.* **2011**, *50*, 9624−9628.
(21) (a) Currie, L. A. *Anal. Chim. Acta* **1999**, *391*, 127−134. (b) Analytical Methods Committee.. *Analyst* **1987**, *112*, 199−204.

dx.doi.org/10.1021/ic402811x | *Inorg. Chem.* 2014, 53, 3012−3021